International Journal for Housing Science and Its Applications
Publish August 10, 2025. Volume 46, Issue 4 Pages 435-443

https://doi.org/10.70517/ijhsa46439

Study on the problem of missing data and treatment strategy in the fault diagnosis of normally direct converter valve

Jianxun Li[1,*], Qi Long[1], Kang Sheng[1], Hao Lai[1], Fengshou Han[1], Teng Peng[1] and Ao Feng[2]
[1] Guangzhou Bureau, Ultra-high Voltage Transmission Company of China Southern Power Grid Co., Ltd., LTD., Guangzhou, Guangdong, 510663, China
[2] Wuhan University, Wuhan, Hubei, 430072, China
Corresponding authors: (e-mail: zlljx001@outlook.com).

Abstract As the core equipment of high-voltage direct current transmission system, the operation reliability of normal direct current converter valve directly affects the stability of power system. In this paper, a composite processing strategy integrating tensor decomposition theory and deep learning is proposed for the fault diagnosis problem under the missing data scenario of normally straight converter valve. A multidimensional data interpolation model is constructed based on Tucker decomposition, and the efficient recovery of high-dimensional missing data is achieved through the co-optimization of core tensor and factor matrix. Design 1DCNN-BiLSTM hybrid network with attention mechanism to enhance the time-frequency characterization of fault features. As verified by the analysis of simulated and measured vibration data on the PSSE platform, the average relative error of the Tucker decomposition and its rate of change are both minimized in the comparison models, and the average MRE is 2.29 in the random missing data scenario. The MRE is reduced by 38.75% compared to the suboptimal model in the PMU fault scenario with 25% high missing rate. The method in this paper can successfully isolate the fault features of severe faults. Moreover, there are rich fault feature modulation bands in addition to the fault feature frequency.

Index Terms normally straight converter valve, Tucker decomposition, deep learning, data interpolation, fault diagnosis

I. Introduction

Normally straight converter valve is the core equipment of DC transmission project, its role is to convert the three-phase AC voltage to the DC side to get the desired DC voltage and realize the control of power, the value of about 22~25% of the total price of the converter station set of equipment, and the process of converting the current is ultimately realized through the thyristor [1]-[4]. The basic component unit of the normally direct converter is the thyristor stage [5]. The thyristor stage consists of a thyristor valve plate, a thyristor voltage monitoring (TVM) plate, an RC damping circuit in parallel with the valve plate, and a DC equalizing resistor mounted in the TVM plate in parallel with the valve plate [6], [7]. However, due to the complex structure and working environment of the normally direct converter valve, its equipment is prone to failures, which bring serious impacts to the power system operation, so the importance of fault diagnosis is self-evident [8]-[10].

Current fault diagnosis methods mainly include model-based methods and machine learning methods [11]. Model-based methods mainly rely on manual empirical judgment or simple rules for fault diagnosis, such as fault tree and state observer methods [12], [13]. Although such methods are able to reason about the causes of faults and locate faulty components from the fault occurrence mechanism, they suffer from strong subjectivity, low diagnostic efficiency, and susceptibility to human factors [14]-[16]. In addition, machine learning-based methods have limited ability to process complex and variable failure modes and large amounts of data, which cannot meet the needs of practical applications [17], [18]. Although these methods can find out the cause of fault occurrence and locate the fault components from the fault occurrence mechanism, but it is easy to cause a large risk of missing data, which will directly affect the accuracy of fault diagnosis, so the study of the data missing problem and processing strategy in the fault diagnosis of the normal direct converter valve is of great significance for the safe operation of the power system [19]-[22].

This paper firstly explains the structural composition and fault mechanism of the normal straight converter valve, analyzes the equivalent circuit of the thyristor assembly and the replacement process. It outlines the application potential of tensor decomposition in power equipment condition monitoring, and proposes a multidimensional data interpolation method based on Tucker decomposition. Construct a fault diagnosis model based on one-dimensional convolutional neural network, bidirectional long and short-term memory and time channel joint attention module. The one-dimensional convolutional neural network is utilized to extract the features of time series data, the two-way

long and short-term memory fully exploits the features of temporal data, and the key information at different times and channels is adaptively learned by the time-channel joint attention module. The effectiveness of the proposed method is verified through simulation and real data, and the interpolation performance and fault classification effectiveness are compared and analyzed. The non-opening and mis-opening faults of the valve are analyzed to reveal the influence of the abnormal triggering pulse of the converter valve on the system voltage.

II. Research on the treatment of missing data and fault diagnosis of normal direct converter valve

As the core technology of long-distance and large-capacity power transmission, the stable operation of high-voltage direct current (HVDC) transmission systems with converter valves is crucial to grid safety. The fault diagnosis of the normally direct converter valve needs to rely on heterogeneous data from multiple sources, including electrical parameters, mechanical vibration and temperature signals, etc. However, in practical engineering, the problem of missing data occurs frequently, resulting in incomplete feature information and reduced robustness of the diagnostic model. Existing research mostly uses interpolation method or single decomposition model to deal with missing data, however, its interpolation accuracy in high-dimensional nonlinear data is limited; at the same time, the traditional fault diagnosis methods are difficult to effectively integrate the temporal features and spatial correlation information, and are susceptible to noise and composite fault interference. Therefore, this paper focuses on two key issues, namely, the repair of missing data and the extraction of fault features, with the aim of constructing an intelligent diagnostic framework for normally direct converter valves.

II. A. Converter valve structure

The current converter valve includes gate unit assembly, thyristor press-fit structure, damping resistor assembly, saturation reactor assembly, damping capacitor assembly, cooling line, DC equalizing resistor, and electrical connection structure. The gate unit assembly, damping resistor assembly, and damping capacitor assembly surround the thyristor press-fit structure. When there is a need for conduction of the current valve, the pulse code is transmitted from the VBE through the fiber optic, and then triggers the thyristor through the TTM decoding, and each thyristor is equipped with a TTM board.

II. A. 1) Thyristor assembly

The equivalent circuit of the thyristor assembly is shown in Fig. 1. R_{dc} is the DC equalizing resistor, R_b is the damping resistor, C_b is the damping capacitor, and TCE is the thyristor control electronics.

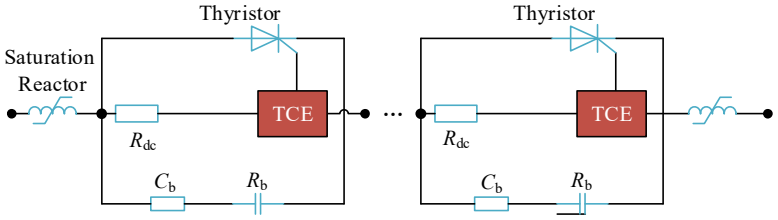

Figure 1: Equivalent circuit of thyristor assembly

The saturated reactor equivalent circuit used in the commutator structure is shown in Fig. 2. C_p is the capacitor impact capacitance, R_{cu} is the reactor coil resistance, R_m is the core resistance and hysteresis loss resistance for eddy current losses, L_m is the core inductance, and L_{air} is the hollow inductance.

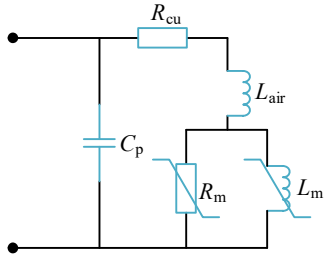

Figure 2: Equivalent circuit of saturated reactor

Analyzing the equivalent circuit of the thyristor assembly and the equivalent circuit of the saturation reactor is conducive to making a quick diagnosis of the converter valve fault, saving the time of fault diagnosis and improving the accuracy of fault location. When analyzing the fault diagnosis method, the thyristor replacement method needs to be analyzed first.

II. A. 2) Thyristor Replacement Methods

Thyristors need to be replaced when they fail badly or have a long service life. Currently, thyristor replacement requires the use of a special tool that relies on silicon stack pressure to repair the thyristor. The tool includes a pressure gauge, a retarder valve assembly, a 25t hydraulic cylinder, a manual hydraulic pump, an adapter assembly, a TCA auxiliary support frame, and a pressure loading plunger.

The manual hydraulic pump oil line has two branches, using only one branch to be able to realize the pressurization or depressurization, when the hydraulic pump completes the work, you can use the other branch to depressurize, using two branches of the hydraulic pump can save the time of replacing the thyristor.

II. B. Tensor Decomposition Theory

In recent years, tensor research has received wide attention in the fields of image processing, service quality prediction, data mining, and traffic flow prediction. In practical applications, due to data acquisition equipment problems, data transmission problems, data storage problems, data processing errors, and data cleaning and screening and other uncontrollable reasons resulting in cyclical missing data, the tensor completion technique needs to be used to recover the missing values by utilizing the acquired data.

II. B. 1) Four-dimensional tensor multiplication

Given that the model presented in this paper is a four-dimensional tensor model, this section focuses on the multiplication of four-dimensional tensors. For the vector spaces V_1, V_2, V_3, V_4 with dimensions I_1, I_2, I_3, and I_4, respectively, the tensor product space $V_1 \circ V_2 \circ V_3 \circ V_4$ in any one of the four-dimensional tensor X is represented as shown in equation (1):

$$X = \sum_{h,j,k,l=1}^{I_1,I_2,I_3,I_4} x_{hjkl} \left(v_{1h} \circ v_{2j} \circ v_{3k} \circ v_{4l} \right) \in R^{(I_1 \times I_2 \times I_3 \times I_4)} \tag{1}$$

where $v_{1h} \circ v_{2j} \circ v_{3k} \circ v_{4l}$ $(1 \le h \le I_1,\ 1 \le j \le I_2,\ 1 \le k \le I_3,\ 1 \le l \le I_4)$ is a set of bases for the tensor product space $V_1 \circ V_2 \circ V_3 \circ V_4$.

For a four-dimensional tensor $X = \left[\left| x_{hjkl} \right| \right] \in R^{I_1 \times I_2 \times I_3 \times I_4}$, the Frobenius-paradigm $\|X\|_F$ is defined as shown in equation (2):

$$\|X\|_F = \sqrt{(X, X)} = \sqrt{\sum_{h=1}^{I_1} \sum_{j=1}^{I_2} \sum_{k=1}^{I_3} \sum_{l=1}^{I_4} x_{hjkl}^2} \tag{2}$$

Let the four-dimensional tensor $X \in R^{I_1 \times I_2 \times I_3 \times I_4}$, matrix $M \in R^{J_n \times I_n}$, any $1 \le n \le 4$ when $n-$ mode tensor X with matrix X the $n-$ mode matrix product $X \times_n M$ is defined as shown in equation (3):

$$\left(X \times_n M \right)_{j_1 \cdots j_{n-1} j i_{n+1} \cdots i_4} = \sum_{i_n=1}^{I_n} x_{i_1 i_2 \cdots i_4} m_{j i_n} \tag{3}$$

where "$\times_n$" denotes the $n-$ pattern matrix product of the tensor, $j = 1, 2, \cdots, j_n$.

The Kronecker product of the tensor X and the matrix M is defined as shown in equation (4):

$$X \otimes M = \left(X_{i_1 i_2 i_3 i_4} \otimes M \right) \in R^{(I_1 J_1) \times (I_2 J_2) \times I_3 \times I_4} \tag{4}$$

where, any $i_n \in I_n$, $n = 1, 2, 3, 4$. When the four-dimensional tensor $X \in R^{I_1 \times I_2 \times I_3 \times I_4}$ is downgraded to a second-order tensor $X \in R^{I_1 \times I_2}$ (i.e., a matrix), the Kronecker product of X and M is the Kronecker product of the matrix.

II. B. 2) Tensor decomposition

The two classical models for tensor decomposition are the Candecomp/Parafac (CP) decomposition and the Tucker decomposition. Compared with the CP decomposition, the core tensor obtained by the Tucker decomposition

requires significantly less storage space, and it is easier to capture the potential connection between the target tensors, and the number of parameters shows an exponential relationship with the order of the tensor, and the time complexity is related to the size of the core tensor, which is more suitable for processing small and medium-sized data.

The Tucker decomposition is the representation of a higher-order tensor as the product of a core tensor and the accompanying matrices corresponding to a number of tensor modes. The process of Tucker decomposition of a third-order tensor is shown in Fig. 3. For any N st order tensor $X \in R^{I_1 \times I_2 \times \cdots \times I_N}$, the Tucker decomposition can be expressed as:

$$X \approx [G; A^{(1)}, A^{(2)}, \cdots, A^{(N)}] = G \times_1 A^{(1)} \times_2 A^{(2)} \times_3 \cdots \times_N A^{(N)} \tag{5}$$

where, the core tensor $G \in R^{J_1 \times J_2 \times \cdots \times J_N}$ retains the main information of the original tensor and $J_N < I_N$, and the factor matrices $A^{(n)} \in R^{I_n \times J_n}$, $(n = 1, 2, \cdots, N)$ represent the principal components of the n th order after decomposition.

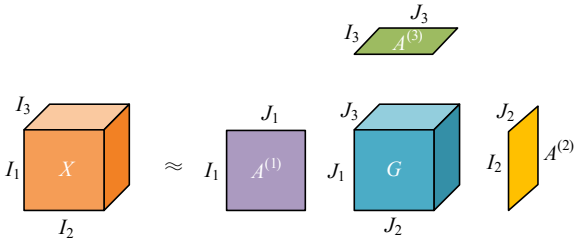

Figure 3: Tucker decomposition of the tensor

II. C.Deep learning based fault diagnosis technique for flexible direct converter valve

II. C. 1) Bidirectional Long and Short-Term Memory Networks

The Bidirectional Long Short-Term Memory Network (BiLSTM) is a sequence model that employs three gate units in order to solve the gradient vanishing problem that occurs in traditional recurrent neural networks. For a given time series $X = [x_1, x_2, \cdots, x_N]$ as an input to the LSTM layer, the LSTM unit computes the t th data $t \in [1:N]$ by the following equation:

$$\begin{cases} i_t = \sigma\left(Linear_i\left(\left[h_{t-1}, x_{t-1}\right]\right)\right) \\ f_t = \sigma\left(Linear_f\left(\left[h_{t-1}, x_{t-1}\right]\right)\right) \\ o_t = \sigma\left(Linear_o\left(\left[h_{t-1}, x_{t-1}\right]\right)\right) \\ \tilde{C}_t = \tanh\left(Linear_c\left(\left[h_{t-1}, x_{t-1}\right]\right)\right) \\ C_t = f_t \square\ C_{t-1} + i_t \square\ \tilde{C}_t \\ h_t = o_t \square\ \tanh\left(C_t\right) \end{cases} \tag{6}$$

where $Linear_k(\cdot)$ denotes the single-layer full linkage, and $k \in \{i, f, o, c\}$ denotes the input gates, oblivion gates, output gates, and cell states, respectively. $H = [h_1, h_2, \cdots, h_N]$ denotes the representation of the encoder's output results at all times.

As shown in Eq. (7), BiLSTM is a model consisting of two LSTMs with opposite directions, where N and d denote the input sample length and output feature length, respectively.

$$H = BiLSTM(X) \in R^{N \times d} = \left[\overrightarrow{LSTM(X)}; \overleftarrow{LSTM(X)}\right]^T \tag{7}$$

Forward LSTM and reverse LSTM are responsible for processing the input sequence data in chronological order and reverse order, respectively, and the flow is shown in Fig. 4. This setup enables the BiLSTM to acquire the before and after timing sequence information before and after the current moment simultaneously. By performing splicing or merging operations on the outputs of forward and reverse LSTMs, we can obtain a representation that comprehensively considers the information of the entire input sequence. This bi-directional modeling approach

allows BiLSTM to better capture the various patterns and regularities present in the time-series data. This modeling is important for revealing the underlying patterns in time-series data.

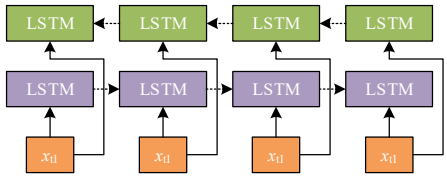

Figure 4: Bidirectional long short term memory network processing data

II. C. 2) Combining 1DCNN-BiLSTM with Attention Module for Fault Diagnosis

The main processes of the fault diagnosis method of 1DCNN-BiLSTM with attention module proposed in this paper are as follows.

(1) Pre-processing process: the one-dimensional voltage signal is augmented and equalized using overlapping sampling method, with 300 samples of each type as a group, and the overlapping step size is based on the number of fault samples of this type.

(2) Feature extraction process: the first layer of the proposed method uses 40 one-dimensional convolution kernels of size 10×1. The second layer uses a temporal channel joint attention module. Among them, the temporal attention module uses one 1D convolutional kernel of size 1×1 and 40 1D depth-separable convolutional kernels of size 5×1 to obtain the importance weights in the temporal dimension; the channel attention module adopts two fully-connected layers of size 5×1 and two fully-connected layers of size 40×1 to assign weights to different channels to assign weights according to their importance.

(3) Classifier: the proposed method uses a global average pooling layer instead of a fully connected layer to simplify the model. Subsequently, the obtained feature maps are input into the Softmax layer for classification, and the model is optimized based on the set loss function, knowing that the number of iterations is reached or the condition of early termination is met. After obtaining the trained model, the performance of the fault diagnosis model is verified by a test set.

III. Data missing treatment and troubleshooting example analysis of normal direct converter valve

III. A. Comparison of interpolation effect of data

Based on the PSSE platform for time-domain simulation, a total of 29,674 transient samples are generated for the 10-machine, 40-node power system in New England, of which 18,853 are stable samples and 10,821 are unstable samples. The interpolation effect of the Tucker decomposition is quantified and compared by calculating the mean relative error (MRE) of the missing data, which is calculated as follows:

$$MRE = \frac{1}{n}\sum_{I=1}^{n}\left|\frac{\tilde{x}_I - \hat{y}_I}{\tilde{x}_I}\right| \tag{8}$$

where $\tilde{x}_I$ and $\hat{y}_I$ are the true and interpolated values of the electrical runs, respectively; n is the sum of the elements of $\bar{M}_t$; MRE is numerically equal to the average of the plausibility R^{P} and R^{F}; and I is the sample size. Random forest (RF) predictor, LSTM predictor, and CP decomposition are introduced to predict or interpolate the missing data.The interpolation effect of Tucker decomposition and comparison model with different missing proportion and different missing types is shown in Fig. 5(a~b).

As the probability of occurrence of missing electrical operation data increases, the interpolation effects of the interpolation models all decrease. The LSTM predictor outperforms the RF predictor in both data missing modes due to the temporal feature extraction capability of the temporal model, and the CP decomposition, although it does not have explicit temporal and spatial feature extraction capability, also exhibits considerable interpolation effects due to its unique mechanism. Overall, the Tucker decomposition achieves the optimal performance by minimizing both the average relative error and its rate of change among the compared models. In the random missing data scenario, the average MRE is 2.29. The Tucker decomposition shows more reliable interpolation for missing feature values due to PMU failures. In the PMU fault scenario with 25% high missing rate, the MRE is only 2.15, which is 38.75% lower than the suboptimal model. The experimental data validate the robustness of the proposed method under complex missing modes, demonstrating its reliability and practicality in engineering applications.

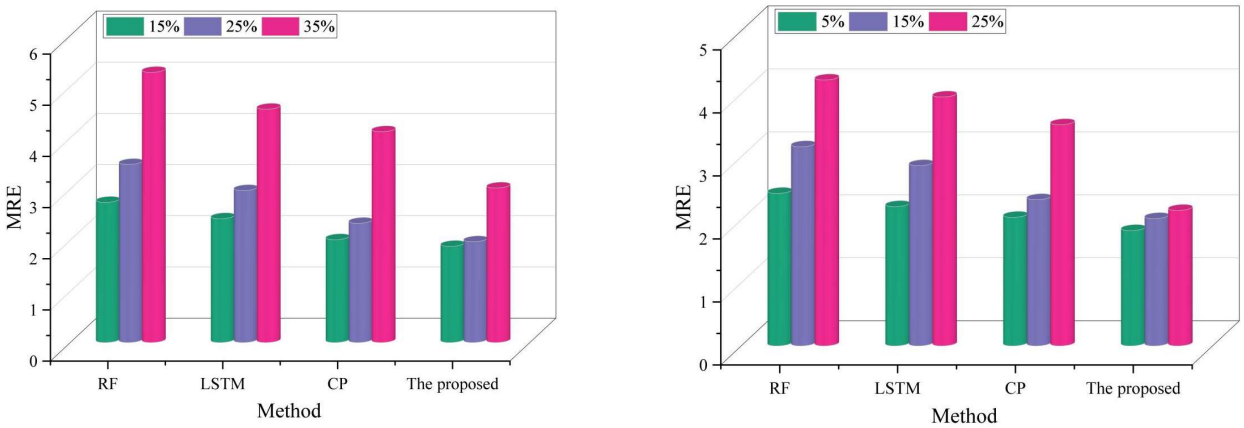

(a)Data missing at random (b)PMU fault

Figure 5: Comparison of prediction or imputation effects of different models

III. B. Troubleshooting Analysis

In this section, the actual vibration data of the converter valve air cooler motor is used as an example to apply the proposed algorithm for validation and assess the effectiveness of the proposed diagnostic method. As the converter valve air cooler works under the environment of humidity, corrosion and external vibration for a long time, it will lead to a high probability of air cooler motor failure and is prone to multiple failures concurrently.

III. B. 1) Validation of validity

In this paper, a magnetic suction vibration sensor is used for data acquisition of the commutator valve air cooler motor, and the time-domain vibration signal x(t) of the bearing measured by the sensor and its frequency domain after FFT are shown in Fig. 6. Among them, the sampling frequency is 15000Hz and the sampling length is 12000 points. In addition, the fault characteristic frequency of the periodic fault is 3 times its rotational frequency, the fault characteristic frequency of the impact fault 1 is about 157.88 Hz, and the fault characteristic frequency of the impact fault 2 is 110.3 Hz. Although there are obvious impact signals in both the time domain and the frequency domain plots, it is not possible to determine the frequency of the faults due to the presence of a large number of resonance spectral peaks in the spectra components.

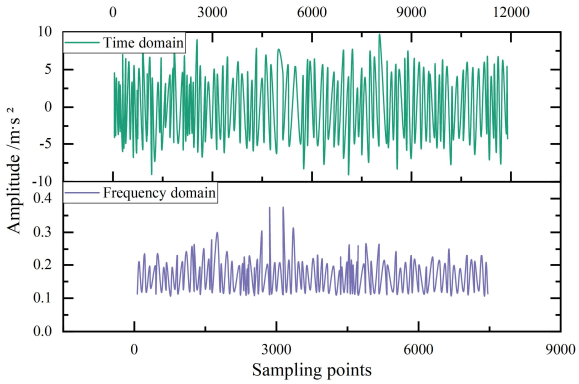

Figure 6: Composite fault time domain and frequency domain

The spectrum of severe fault feature 1 obtained using the method of this paper is shown in Fig. 7. The method of this paper can successfully isolate the fault features of severe faults. Moreover, in addition to the fault feature frequency f_{n1} and its multiplier frequencies $2f_{n1}$,, $3f_{n1}$, there are rich modulation bands of fault features. Similarly, fault feature 2 can be well recognized, thus verifying the effectiveness of the proposed method.

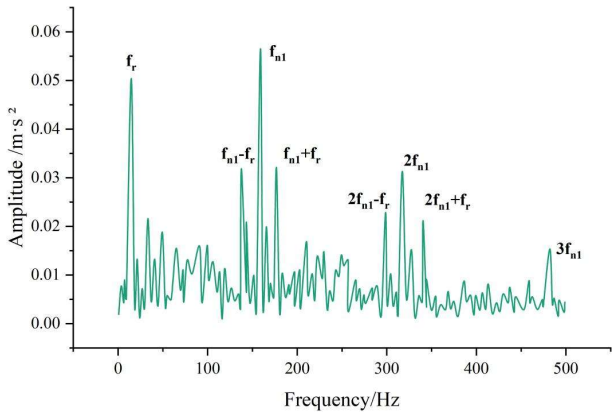

Figure 7: Spectrum of severe fault feature 1

III. B. 2) Troubleshooting

The proposed method is further used to investigate the voltage RMS situation when the non-opening and mis-opening faults occur in the converter valve. When the valve does not turn on, take the converter valve system V1 as an example, the RMS voltage waveform of the system's commutated phase is shown in Fig. 8. After the loss of the V1 trigger pulse, V1 cannot conduct normally, V5 fails to commutate to V1, and V5 continues to turn on, at which time V1 is subjected to a positive voltage. Other valves conduct normally, after V2 conducts, causing a short circuit on the DC side, the fault continues until V3 conducts and disappears, after which the system enters the normal state.

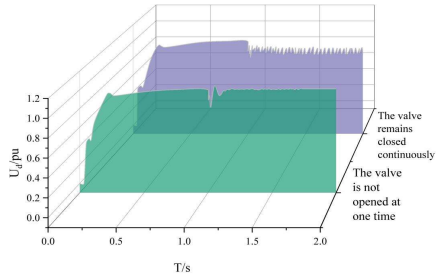

Figure 8: Effective value of fault commutation voltage without valve opening

When the valve is mistakenly turned on, take the converter valve system V1 as an example, the RMS phase voltage waveform of the system is shown in Fig. 9. when the trigger pulse of V1 persists, i.e., when V1 continues to conduct, it causes a short-circuit on the DC side after V4 conducts until the fault disappears in the cycle after V4 shuts off and V6 turns on, and the fault repeats itself afterward, resulting in a decrease in the RMS phase-voltage and cyclical fluctuations. Compared with the normal case, the inverter side is controlled by constant current, but the trans-advance trigger angle increases and periodic continuous fluctuation occurs. The case of pulse advance triggering is only equivalent to an increase in the trigger angle of the valve, which has a very small effect on the system as can be seen from the voltage RMS waveform shown in Fig. 9.

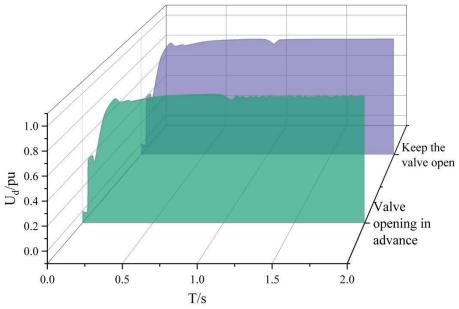

Figure 9: Effective value of fault commutation voltage without valve opening

The analysis results show that when the valve is triggered early, the effect on the system is small and usually negligible. When the loss of a single trigger pulse causes the valve to turn on incorrectly, the system returns to normal operation after a short transient process. When the valve is continuously turned on and continuously not turned on, the RMS value of the system commutation voltage decreases and fluctuates periodically, but the latter is more serious than the former.

IV. Conclusion

Aiming at the fault problem of the normally direct converter valve, this paper proposes to use Tucker decomposition to deal with the problem of missing data, and designs a fault diagnosis method that combines 1DCNN-BiLSTM with the attention module.

Based on the time-domain simulation of the PSSE platform, the interpolation effects of the interpolation models are all reduced with the increase of the probability of the occurrence of missing electrical operation data.The average relative error of the Tucker decomposition and its rate of change are both minimized among the comparison models, and the optimal performance is achieved. In the random missing data scenario, the average MRE is 2.29. The Tucker decomposition shows more reliable interpolation for missing feature values due to PMU failures. In the PMU fault scenario with 25% high missing rate, the MRE is only 2.15, which is 38.75% lower than the suboptimal model. The experimental data validate the robustness of the proposed method under complex missing modes, demonstrating its reliability and practicality in engineering applications.

Taking the actual vibration data of the air cooler motor of the converter valve as an example, the method in this paper can successfully isolate the fault characteristics of serious faults. Moreover, there are rich modulation bands of fault features in addition to the fault feature frequency, which verifies the effectiveness of the proposed method. For the occurrence of non-opening and mis-opening faults of the converter valve, the analysis results show that when the valve is triggered in advance, the impact on the system is small and usually negligible. When the loss of a single triggering pulse leads to valve misopening, the system returns to normal operation after a short transient process. In the case of sustained valve turn-on and sustained non-turn-on, the RMS value of the system commutation voltage decreases and fluctuates periodically, but the latter is more serious than the former.

Funding

This work was supported by the Science and Technology Project of China Southern Power Grid Company Limited under (CGYKJXM20220335).

References

[1] Qi, L., Wang, M., Zhang, X., Shen, H., Wang, H., & Jiao, C. (2023). Analysis for magnetic field disturbance of modular multilevel converter based high voltage direct current (MMC-HVDC) converter valve. High Voltage, 8(1), 91-101.

[2] Cao, J., Ji, F., Liu, J., & Chen, P. (2016). Valve saturable reactor iron losses of ultrahigh-voltage direct current converter. IET Science, Measurement & Technology, 10(2), 77-83.

[3] Chen, Z. H. O. U., Qiang, Z. H. O. U., Yeyuan, X. I. E., Yu, L. U., Taixun, F. A. N. G., & Wenxin, Z. H. A. O. (2025). High-voltage Self-energy Gaining Technology for the Driving Power Supply of Novel High-voltage Direct Current Converter Valve. High Voltage Engineering, 51(3), 1307-1317.

[4] Wang, X., Liu, X., Wang, C., Liu, N., Jiao, X., & Liu, L. (2015, October). Numerical calculation of current through grading electrodes in inner cooling circuit of HV converter valve. In 2015 IEEE Conference on Electrical Insulation and Dielectric Phenomena (CEIDP) (pp. 411-414). IEEE.

[5] Liu, Y., Lai, T., Liu, J., Wei, X., Pei, S., Wang, C., & Zhang, X. (2022). Vibration detection method for core loosening degree of high-voltage direct current converter valve saturable reactor based on variational mode decomposition-symmetrized dot pattern and image matching. IET Science, Measurement & Technology, 16(8), 454-466.

[6] Sun, R. C., Wang, Z., Klebanov, M., Liang, W., Liou, J. J., & Liu, D. G. (2015). Silicon-controlled rectifier for electrostatic discharge protection solutions with minimal snapback and reduced overshoot voltage. IEEE Electron Device Letters, 36(5), 424-426.

[7] Zhu, Z., Yu, G., Yang, S., Xu, L., Yang, Z., Wang, T., ... & Garistov, V. (2025). A vertical diode-triggered silicon-controlled rectifier with adjustable holding voltage for ESD protection. Microelectronics Reliability, 167, 115631.

[8] Ji, Y., Yuan, Q., Zhou, C., Yang, M., Huang, X., Ma, L., & Zhao, H. (2025). Analysis of the Impact of Short Circuit Faults in Converter Valve Submodules on Valve Power Transmission. Energies, 18(6), 1496.

[9] Xiao, K., Wang, Z., Zou, Y., Liang, N., Xu, H., & Ji, K. (2022, December). Fault Analysis of Converter Valve Power Module in Flexible Direct Current Transmission. In Frontier Academic Forum of Electrical Engineering (pp. 1189-1200). Singapore: Springer Nature Singapore.

[10] Yanxia, Z. H. A. N. G., Yue, H. A. N., Yachao, C. H. E. N. G., & Kaixiang, L. I. U. (2021). Fault analysis for valve side winding of converter transformer. Power System Technology, 46(7), 2794-2803.

[11] Yin, S., & Li, X. (2023). Converter valve-level fault location method based on the temporal differences among horizontal and longitudinal valve states. International Journal of Electrical Power & Energy Systems, 154, 109458.

[12] Aviña-Corral, V., de Jesus Rangel-Magdaleno, J., Barron-Zambrano, J. H., & Rosales-Nuñez, S. (2024). Review of fault detection techniques in power converters: Fault analysis and diagnostic methodologies. Measurement, 114864.

[13] Poon, J., Jain, P., Konstantakopoulos, I. C., Spanos, C., Panda, S. K., & Sanders, S. R. (2016). Model-based fault detection and identification for switching power converters. IEEE Transactions on Power Electronics, 32(2), 1419-1430.
[14] Venkata, S. K., & Rao, S. (2019). Fault detection of a flow control valve using vibration analysis and support vector machine. Electronics, 8(10), 1062.
[15] Xiong, F., Cao, C., Tang, M., Wang, Z., Tang, J., & Yi, J. (2022). Fault detection of UHV converter valve based on optimized cost-sensitive extreme random forest. Energies, 15(21), 8059.
[16] Zhou, S., Qin, L., Sun, H., Peng, B., Ruan, J., Wang, J., ... & Liu, K. (2023). TransFNN: A Novel Overtemperature Prediction Method for HVDC Converter Valves Based on an Improved Transformer and the F-NN Algorithm. Sensors, 23(8), 4110.
[17] Utah, M. N., & Jung, J. C. (2020). Fault state detection and remaining useful life prediction in AC powered solenoid operated valves based on traditional machine learning and deep neural networks. Nuclear Engineering and Technology, 52(9), 1998-2008.
[18] Dutta, N., Kaliannan, P., & Subramaniam, U. (2020). Application of machine learning algorithm for anomaly detection for industrial pumps. In Machine Learning Algorithms for Industrial Applications (pp. 237-263). Cham: Springer International Publishing
[19] Sun, F., Xu, H., Zhao, Y. H., & Zhang, Y. D. (2022). Data-driven fault diagnosis of control valve with missing data based on modeling and deep residual shrinkage network. Journal of Zhejiang University-SCIENCE A, 23(4), 303-313.
[20] Subbaraj, P., & Kannapiran, B. (2014). Fault detection and diagnosis of pneumatic valve using Adaptive Neuro-Fuzzy Inference System approach. Applied Soft Computing, 19, 362-371.
[21] Maalla, A. (2019, March). Research on Fault Diagnosis of Fieldbus State in Converter Station. In 2019 IEEE 3rd Information Technology, Networking, Electronic and Automation Control Conference (ITNEC) (pp. 2553-2557). IEEE.
[22] Liu, Y. K., Zhou, W., Ayodeji, A., Zhou, X. Q., Peng, M. J., & Chao, N. (2021). A multi-layer approach to DN 50 electric valve fault diagnosis using shallow-deep intelligent models. Nuclear Engineering and Technology, 53(1), 148-163.